Carderock Division,
Naval Surface Warfare Center

Bethesda, Maryland 20084-5000

CRDKNSWC/HD-1282-01 AUGUST 1996

Hydromechanics Directorate
Research and Development Report

PROPELLER CAVITATION PREDICTION FOR A SHIP IN A SEAWAY

BY

STUART D. JESSUP AND HAN-CH'ING WANG

PROPELLER CAVITATION PREDICTION FOR A SHIP IN A SEAWAY

CRDKNSWC/HD-1282-01

MAJOR DTRC TECHNICAL COMPONENTS

CODE 011 DIRECTOR OF TECHNOLOGY, PLANS AND ASSESSMENT

12 SHIP SYSTEMS INTEGRATION DEPARTMENT

14 SHIP ELECTROMAGNETIC SIGNATURES DEPARTMENT

15 SHIP HYDROMECHANICS DEPARTMENT

16 AVIATION DEPARTMENT

17 SHIP STRUCTURES AND PROTECTION DEPARTMENT

18 COMPUTATION, MATHEMATICS & LOGISTICS DEPARTMENT

19 SHIP ACOUSTICS DEPARTMENT

27 PROPULSION AND AUXILIARY SYSTEMS DEPARTMENT

28 SHIP MATERIALS ENGINEERING DEPARTMENT

DTRC ISSUES THREE TYPES OF REPORTS:

1. **DTRC reports, a formal series,** contain information of permanent technical value. They carry a consecutive numerical identification regardless of their classification or the originating department.

2. **Departmental reports, a semiformal series,** contain information of a preliminary, temporary, or proprietary nature or of limited interest or significance. They carry a departmental alphanumerical identification.

3. **Technical memoranda, an informal series,** contain technical documentation of limited use and interest. They are primarily working papers intended for internal use. They carry an identifying number which indicates their type and the numerical code of the originating department. Any distribution outside DTRC must be approved by the head of the originating department on a case-by-case basis.

REPORT DOCUMENTATION PAGE

Form Approved
OMB No. 0704-0188

1. AGENCY USE ONLY (Leave blank)	2. REPORT DATE	3. REPORT TYPE AND DATES COVERED
	August 1996	Final; October 1994 thru December 1995

4. TITLE AND SUBTITLE
PROPELLER CAVITATION PREDICTION FOR A SHIP IN A SEAWAY

5. FUNDING NUMBERS
PE : 06D2121
PR : RB2133-MSI
WU : 1-5060-544

6. AUTHOR(S)
Stuart D. Jessup and Han-Ch'ing Wang

7. PERFORMING ORGANIZATION NAME(S) AND ADDRESS(ES)
Hydromechanics Directorate, Code 5400
Carderock Division
Naval Surface Warfare Center
Bethesda, MD 20084-5000

8. PERFORMING ORGANIZATION REPORT NUMBER
CRDKNSWC/HD-1282-01

9. SPONSORING/MONITORING AGENCY NAME(S) AND ADDRESS(ES)
Office of Naval Research (334)
800 N. Quincy Street
Arlington, VA 22217-5000

10. SPONSORING/MONITORING AGENCY REPORT NUMBER

11. SUPPLEMENTARY NOTES

12a. DISTRIBUTION/AVAILABILITY STATEMENT
APPROVED FOR PUBLIC RELEASE.
DISTRIBUTION UNLIMITED.

12b. DISTRIBUTION CODE

13. ABSTRACT *(Maximum 200 words)*

A computational procedure has been developed to predict the influence of ship motions in waves on propeller cavitation inception. A test case has been performed on the DD963 hull form and propeller predicting the influence of various sea states on propeller cavitation inception. Simple modifications of the propeller geometry were made to assess the potential of improving propeller cavitation performance with consideration of design trade-offs.

14. SUBJECT TERMS
Propeller Cavitation, Ship Motion

15. NUMBER OF PAGES
iv + 20

16. PRICE CODE

17. SECURITY CLASSIFICATION OF REPORT	18. SECURITY CLASSIFICATION OF THIS PAGE	19. SECURITY CLASSIFICATION OF ABSTRACT	20. LIMITATION OF ABSTRACT
UNCLASSIFIED	UNCLASSIFIED	UNCLASSIFIED	Same as Report

CONTENTS

FIGURES

TABLES

NOTATION

A	Wave single amplitude
C_p	pressure coefficient, $(p-p_0)/ 1/2\rho V_s^2$
C_{pmin}	Minimum pressure coefficient
D	Propeller diameter
H	Significant Wave height
K_t	Thrust coefficient, $K_t = T/(\rho n^2 D^4)$
J_a	Advance coefficient, $V_a/(nD)$
r	Local propeller radius
R	Ship resistance
T	Propeller thrust
ϕ_1	First harmonic, time domain, phase angle at the propeller plane due to seaway
θ	Angular position at propeller plane, degrees, 0 @TDC
V_t	Tangential velocity of the propeller wake
V_x	Axial velocty in the propeller plane
V_r	Radial velocity in the propeller plane
Vs	Ship Speed
Va	Volume average effective axial velocity at propeller plane

Subscripts

ave	Circumferential average
c	captive, waves, but no hull motion
f	free, waves and hull motion
peak, ave	Average peak
cw	Calm Water
min	Value producing minimum loading
max	Value producing maximum loading
t	Tangential
x	Axial
r	Radial
SS	Sea State
1	First spatial harmonic at the propeller plane

ABSTRACT

A computational procedure has been developed to predict the influence of ship motions in waves on propeller cavitation inception. A test case has been performed on the DD963 hull form and propeller predicting the influence of various sea states on propeller cavitation inception. Simple modifications of the propeller geometry were made to assess the potential of improving propeller cavitation performance with consideration of design trade-offs.

ADMINISTRATIVE INFORMATION

This report is submitted in partial fulfillment of milestone 2, Propulsor Design Methodology, of task 4, Effects of Sea State, in the Advanced Propulsion Systems Project (RB2133-MS1), in the Surface Ship Technology Program Plan (Program Element 0602121) for fiscal year 1995. The work described herein was sponsored by the Office of Naval Research (ONR 334) and performed by the Carderock Division, Naval Surface Warfare Center, Code540 under Work Unit Number 1-5060-554.

INTRODUCTION

In recent years, there has been increasing interest in the consideration of propeller performance when operating in a typical seaway. In some cases, Navy propeller design requirements determined by NAVSEA have included propeller cavitation inception with ship operation in a seaway. An example was in the design of an Oceanographic Research Ship, T-AG(X)[1](1989) where operation in extreme sea states was considered by applying margins to the still water cavitation predictions.

With present predictive tools for the motion of a ship in a seaway, it was appropriate to develop a numerical procedure to calculate the time varying flow field into the propeller disk due to a ship operating in regular waves and calculate the effect of the unsteady flow field on propeller performance. This procedure is potentially an improvement over less accurate estimations of ship motions and wave orbital velocities. The procedure used for predicting the ship motion in regular waves was the SWAN[2](Ship Wave Analysis) code. This code is potential based, and solves the complete 3D potential problem. The code output was interpreted to calculate the time varying

velocity at the propeller plane by Kim and Chevalier[3]. The propeller performance was calculated in a quasi steady fashion using a potential based panel code[4].

The usefulness of an improved prediction capability is to provide the designer the ability to consider the influence of the ship in a seaway in the overall requirements of the design. A sample design exercise was performed to illustrate design trade-offs that can be performed.

PREDICTION OF PROPELLER INFLOW DUE TO WAVES AND SHIP MOTION

The prediction of propeller inflow due to waves and ship motion was performed using the MIT SWAN[2] code. The output of the code was modified by Kim and Chevalier[3] to compute the time varying velocity in the propeller disk. The entire code was run on a workstation with cases running about 15 minutes. The calculation procedure was validated by comparing with measured propeller plane velocity obtained by Aalbers and van Gent[5]. Both captive and free model cases were compared, with the captive case correlating well, while the free model case over predicted the magnitude of the measured velocities. This implies that for the free model case, which is of interest for the actual design problem, the prediction method will produce a conservative estimate of the effect of the freely pitching and heaving ship in a seaway.

Calculations were performed on the DD963 hull form operating in regular ahead seas. The full scale ship length is 520 feet(162M), which was operated at 20 kts in regular waves of length equal to ship length, with wave amplitudes of 0.6, 1, and 2.5M, which represented significant wave heights corresponding to sea states 3,4, and 5. In the wave amplitude range investigated, it was found that the perturbation velocities in the propeller plane were linear in magnitude with wave amplitude. Consequently, future calculations would require only one wave height calculation, with assumed linear behavior up to at least a wave amplitude/ship length equal to 0.015.

VELOCITY VARIATION AT THE PROPELLER PLANE

The velocity variation at the propeller plane was represented as a first harmonic amplitude with wave frequency at specified radial and circumferential locations in the propeller plane. The axial and tangential velocity was considered dominant in altering the propeller loading. Table 1 shows the tabulated perturbation velocities for the 1 meter wave case.

Figure 1 shows the calculated variation in the first harmonic amplitude of velocity as a function of angular location in the propeller disk at r/R=0.57 for the free model case. The axial velocity, $V_{x,1}$, is relatively constant through the propeller plane, with some increase in velocity

perturbation at the top of the disk, presumably due to the influence of the hull. The tangential velocity shows a large variation with angle, which is primarily a geometric effect. The vertical velocity is the primary lateral flow variation, which is also relatively constant through the disk. When represented in the cylindrical coordinate system of the propeller, as a tangential velocity it shows a once /revolution variation. When shown as the first harmonic amplitude, it results in peak values at the sides of the disk, 90 and 270 degrees.

From inspections of other radii along with that shown in Fig. 1, the following assumptions were made to simplify the representation of the velocity perturbation due to waves and ship motion.

1. The axial perturbation velocity at each propeller radii is assumed constant , represented as the calculated radial average, $(V_{x,1})_{ave}$

2. The tangential perturbation velocity, is represented as the average of the maximum values on each side of the disk, $(V_{t,1})_{peak,ave}$.

3. The phase between the axial and tangential velocity perturbations, is assumed to be 90 degrees, thus permitting independent assessments of their effects on cavitation performance.

The table below shows the amplitudes and time domain phase angles of the first harmonic of velocity due to the waves and ship motion.

@0.57R	$(V_{x,1})_{ave}/Vs$	$\phi_{1,vx}$ (degrees)	$(V_{t,1})_{peak,ave}/Vs$	$\phi_{1,vt}$ (degrees)	$\Delta\phi$
Captive model	0.039	-146	0.0235	-58	88
Free model	0.0516	-155	0.049	-85	70

For the captive case, the axial and tangential velocity are very close to 90 degrees out of phase. For the free model case, this is less of the case. To simplify the analysis , the velocity components are treated independently. This assumption could reduce the peak influence of the waves for the free model case by

$$1 / (1+ \sin(70°)) = 0.75$$

When performing an analysis for a specific application, then relative phase between the two components of velocity could be easily accounted for.

At each radial location the effect of waves and ship motion is represented by a perturbation of the still water wake by $(V_{x,1})_{ave,}$ and $(V_{t,1})_{peak,\ ave}$. Figure 2 shows the variation of these quantities with radius for the 1 m wave case. Also shown is the calm water first harmonic tangential velocity. First to be noted is that the 1 meter wave case does clearly present a perturbation to the still water case, since the tangential velocity is about 1/3rd its value. The increase in the tangential velocity for the still water case near the root of the propeller is due to flow augmentation from the upstream shaft. The calculation performed using the SWAN code neglect the shafting and show no augmentation at the inner radii. Also note that the free model case produces larger velocity perturbations that the captive case.

ADDED RESISTANCE

The effect of waves and ship motion on the time average performance of the propeller is a very important component of the propeller load augmentation. This aspect unfortunately is not addressed numerically in this procedure. A simple empirical approach was used to predict added resistance for the combatant hull form investigated. Data from Lloyd[5], shown in Figure 3, was used to develop multiplicative factors to be applied to calm water resistance for effects of wind and waves in head seas. Figure 4 shows the variation in added resistance for the three sea states considered. The table below shows the multiplicative factors used from Figure 4. A very large effect of speed is seen in the figure, with a large increase in resistance at low speed at high sea states.

SEA STATE	10 KTS	15 KTS	20 KTS	25 KTS	30 KTS	32 KTS
3	1.131	1.085	1.047	1.033	1.025	1.023
4	1.335	1.219	1.12	1.085	1.064	1.06
5	3.29	2.13	1.52	1.35	1.235	1.216

Multiplicative factor, M, where, $R_{SS} = M * R_{calm\ water}$

For reference purposes, the following table relates the various wave height parameters investigated.

reg. wave amplitude, A (m)	significant wave height,(m) $H = 2A/\sqrt{2}$	Assumed Sea State	NATO Sea State Standard, Significant Wave Height(m) for assumed sea state
0.62	0.88	3	0.88
1	1.4	4	1.88
2.5	3.54	5	3.25

CALCULATION OF MEAN PROPELLER OPERATING CONDITION IN WAVES

From the added resistance, calm water resistance, and the open water performance of the propeller, the operating advance coefficient, J_a, was calculated for use in the propeller cavitation predictions. The procedure is as follows. Provided from powering data, EHP, augmented by the sea state, and (1-t) are specified for measured speed. The speeds at which calculations were made were 10, 15, 20, 25, 30, and 32 knots. Thrust per shaft for this twin shaft configuration is,

$$T\ (lb.) / shaft = (M*326*EHP_{total}) / (2\ Vs\ (1-t)), \qquad V_s \text{ in kts}$$

To obtain the operating point, K_t/Ja^2 is calculated and plotted against the open water K_t verses J.

$$K_t / J_a^2 = T / \rho D^2 V^2$$

$$\text{plotting}, K_t = (K_t / J_a^2)\ J^2$$

Figure 5 shows a sample of this graphical process for determining the propeller advance coefficient, J_a, for various speeds.

A straightforward calculation of cavitation number, σ, was made through the speed range of the propeller.

$$\sigma = (2gH) / V_S^2, \text{ where H is the depth of submergence in calm water}$$

EFFECTS OF SEAWAY ON CAVITATION INCEPTION

The cavitation inception prediction method utilizes wake predictions along with propeller panel method calculations to predict the blade pressure distribution and thus the minimum blade surface pressure, and the propeller cavitation inception index, where,

$$\sigma_i = -(C_{pmin}) \text{ calculated w/ panel method}$$

WAKE INPUT

The propeller inflow wake used in the calculations included an idealized calm water (cw) wake, and the perturbation velocities due to waves and ship motion superimposed upon the calm water inflow. The calm water, circumferential average wake was idealized as follows,

$$V_x = 1.0, \; V_t = 0.0, \; V_r = 0.0, \quad \text{for all values of r/R}$$

The maximum and minimum loading conditions of the propeller blade due to the calm water blade inflow variations were idealized by considering the flow inclination, only, as follows,

$$V_t(r)_{cw,max} = V_{t,1}(r), \qquad V_t(r)_{cw,min} = -V_{t,1}(r)$$

Where $V_{t,1}(r)$ is obtained from a standard, straight ahead, calm water wake survey[6].

The wave and ship motion induced perturbation velocities were added to the calm water wake in a fashion to create the four independent extremes in propeller loading as follows, for the captured (c) and free (f) model cases.

1. maximum loading due to axial velocity ,

$$V_x(r)_{max,c,f} = 1.0 - (V_{x,1}(r)_{ave})_{c,f} \quad , \quad V_t(r) = V_{t,1}(r)_{cw}, \quad V_r = 0.0$$

2. minimum loading due to axial velocity ,

$$V_x(r)_{min,c,f} = 1.0 + (V_{x,1}(r)_{ave})_{c,f} \quad , \quad V_t(r) = -V_{t,1}(r)_{cw}, \quad V_r = 0.0$$

3. maximum loading due to tangential velocity,

$$V_x(r) = 1.0 \quad , \quad V_t(r)_{max,c,f} = V_{t,1}(r)_{cw} + V_{t,1}(r)_{peak,ave,\ c,f} \quad , \quad V_r = 0.0$$

4. minimum loading due to tangential velocity ,

$$V_x(r) = 1.0 \quad , \quad V_t(r)_{min,c,f} = -V_{t,1}(r)_{cw} - V_{t,1}(r)_{peak,ave,\ c,f} \quad , \quad V_r = 0.0$$

For the DD-963 hull, the components necessary to construct the above propeller inflow wakes are as follows.

	$V_{x,1}(r)_{ave}$		$V_{t,1}(r)_{peak,ave}$		
r/R	captive	free	captive	free	calm water
0.37	0.038	0.0502	0.0235	0.049	0.178
0.57	0.039	0.0516	0.0235	0.049	0.129
0.8	0.040	0.0569	0.0240	0.049	0.128
1.0	0.042	0.0561	0.0265	0.049	0.120

PROPELLER PANEL METHOD

A panel method is used to calculate the time varying propeller blade pressure distribution. The code used, PSF10[4], calculates the steady blade pressure distribution, assuming uniform steady inflow. Both the hull and wave motion is assumed low frequency relative to the propeller rotation rate, therefore, the effects of seaway is considered in a quasi-steady fashion. The extreme wake inflows presented in the previous section are calculated as if the flow was circumferentially uniform and time independent.

A further quasi-steady assumption has been made to simplify the analysis. The primary unsteady flow for the calm water case is due to the propeller shaft inclination, causing a once per revolution blade section angle of attack variation. The reduced frequency of the blade unsteady load is low, permitting a further quasisteady assumption in the propeller analysis of the primary shaft inclination wake. The effects of the shaft and struts are ignored which is consistent with computation of the inflow effects of waves and ship motion.

These assumptions, along with the wake details described in the previous section, and the propeller geometry were sufficient to perform the cavitation inception analysis. Because the free model case was more representative, and resulted in larger effects on cavitation, the free model case was predicted, the captive model case was not.

The panel method has been demonstrated to predict the cavitation inception performance of blade surface , and root cavitation[7]. The prediction of tip vortex was not as accurate, but is thought sufficient to predict trends in tip vortex inception. The paneling used to calculated the blade pressure distribution is shown in Fig. 6. A 30 by 50 grid is used on the blade as a reasonable trade-off between spatial blade resolution and run time (approx. 10 minutes). Root and tip cavitation inception were identified by the minimum pressure occurring at the nearest panels to the hub and the outer chordwise row of tip panels. Blade surface cavitation was identified by minimum pressure calculated amonst the remaining panels, generally occurring at the blade leading edge. Calculations were performed over a range of J, about the operating J's calculated at the calm water condition and the included added resistance. A typical panel method output summary is reproduced in Table 2, which also shows the propeller input geometry.

In the present analysis, there was no consideration of variation in the static pressure at propeller plane. The head was assumed constant at the still water propeller shaft axis value, independent of waves, hull motion and propeller angular location.

REPRESENTATION - CAVITATION INCEPTION CURVES

Cavitation inception curves were prepared resembling a traditional cavitation performance diagram. The propeller cavitation number for operating points through the speed range was plotted verses the advance coefficient, J. Also plotted was the cavitation inception curves for the various types of cavitation, suction and pressure side leading edge (SSLE, PSLE), suction and pressure side root, suction side and pressure side tip vortex(SSTV, PSTV). For this study, the predicted inception speeds were obtained graphically.

Fig. 7 shows the cavitation inception prediction for the effects of added resistance only. In the figure only the propeller operating points change with increasing wave height. Very significant reductions in cavitation inception speed occur for the suction side inception with the reduction in advance coefficients with increased sea state. Also shown is a comparison of SSTV prediction from model test data and predictions using the method described. Obviously for tip vortex, only trends can be predicted with this method.

Fig. 8a shows the cavitation diagram for 1 meter amplitude waves with free motion, representing sea state 4. Only the suction side cavitation is shown since pressure side cavitation is not degraded. It is clear that the cavitation most effected is tip vortex, then blade surface and lastly root cavitation Fig. 8b shows the similar diagram for the SS3, 0.6 meter wave amplitude case. Both curves show that the axial velocity perturbation has a larger effect than the tangential velocity.

Fig. 9 plots the cavitation inception speeds, in knots, predicted as a function of significant wave height. As mentioned earlier, the largest effect occurs with tip vortex, the least with root cavitation. Again, it should be noted, that these predictions do not include wakes from the shaft and struts, which could result in higher predicted inception speeds than is typical for model or full scale data.

CONSIDERATION OF SEAWAY EFFECTS IN PROPELLER DESIGN

With the procedures presented above, predictions of cavitation inception in a seaway can be estimated. Consideration of seaway performance can be included in the overall design of the propeller.

An exercise was conducted to perform a propeller design iteration investigating effects of geometry changes on the cavitation performance in a seaway. A primary parameter effecting cavitation inception is blade thickness. Fig. 10 depicts a variant of the original propeller thickness to chord ratio. Using the same sea state 4 propeller inflow variation as previously discussed, panel calculations were performed, along with calm water calculations. Fig. 11 shows the blade surface leading edge cavitation inception diagram for calm water and sea state 4, due to axial inflow variations. The modified propeller shows only a slight improvement of 0.2 knots inception speed in calm water , with a 1 knot improvement in sea state 4.

A noticeable improvement is observed in inception speed , but there is a design trade-off of increased risk of thrust breakdown at higher speeds. Fig. 12 shows the calculated mid-span blade pressure distribution at high loading due to axial variations in the inflow wake. At the blade leading

edge, a reduction in the suction peak is seen. Mid-chord, a 1 knot loss in back bubble cavitation inception is shown. Qualitatively, thrust breakdown will occur about 1 knot earlier with the thicker blade.

CONCLUSIONS

A prediction method has been developed for propeller cavitation inception in a seaway. The method is based on potential flow calculation of the flow around a hull in a seaway free to pitch and heave. The propeller inception calculations are performed using a quasisteady, potential based panel method.

Calculations were performed for a surface ship transom stern, frigate type combatant hull form operating in regular, ahead seas. Wave amplitudes corresponding to sea states 3, 4 and 5 were investigated. The following conclusions were reached.

1. The hull form, seaway calculations and the propeller panel method calculations were *not* computationally burdensome, and would be appropriate for use in the propeller design.
2. Of the flow variations calculated at the propeller disk, the axial velocity variations were somewhat larger that the tangential velocities, and resulted in a larger effect on cavitation inception speed.
3. Of the three forms of cavitation predicted, the loss in inception speed due to seaway is largest for tip vortex, then blade surface, and least for root cavitation.
4. The prediction of inception speed lost as a function of wave height could be considered typical for transom stern combatant hull forms.
5. Propeller modifications to improve seaway cavitation performance must be traded off against adverse effects of cavitation at high speeds, such as thrust breakdown.

ACKNOWLEDGMENTS

The authors would like to thank Dr. Yoon-Ho Kim for performing the ship motion calculations with the SWAN program, used for the cavitation predictions presented in this report.

REFERENCES

1. Kim, K-H, and Bailar, J.W., "Preliminary Propeller Design and Performance Prediction for Oceanographic Research Ship, T-AG(X)," David Taylor Research Center report, DTRC/SHD-1295-02, April 1989.

2. Sclavounos, P. and Nakos, D. , "Ship Motions by a Three-Dimensional Rankine Panel Method," 18th Symposium on Naval Hydrodynamics, U.S.A., 1991.

3. Kim, Y-H, and Chevalier, Yves, " Propeller Working in a Seaway," PRADS'95 Symposium, Seoul, Korea, September 1995.

4. Hsin,C-Y., Kerwin, J.E., and S.A. Kinnas, "A Panel Method for the Analysis of Flow Around Highly Skewed Propellers," SNAME Propeller and Shafting '91 Symposium, Virginia Beach, Virginia, 1991.

5. Lloyd, A.R.J.M., Seakeeping: Ship Behaviour in Rough Weather, Ellis Horwood Limited, Chichester, U.K.

6. Jessup, S.D., R.J. Boswell, J.J. Nelka, " Experimental Unsteady and Time Average Loads on the Blades of the CP Propeller on a Model of the DD-963 Class Destroyer for Simulated Modes of Operation," DTNSRDC Report 77-0110, December 1977.

7. Jessup, S.D., W. Berberich, K. Remmers, " Cavitation Performance Analysis of Naval Surface Ship Propellers with Standard and New Blade Sections." 20th Symposium on Naval Hydrodynamics, Santa Barbara, California, 1994.

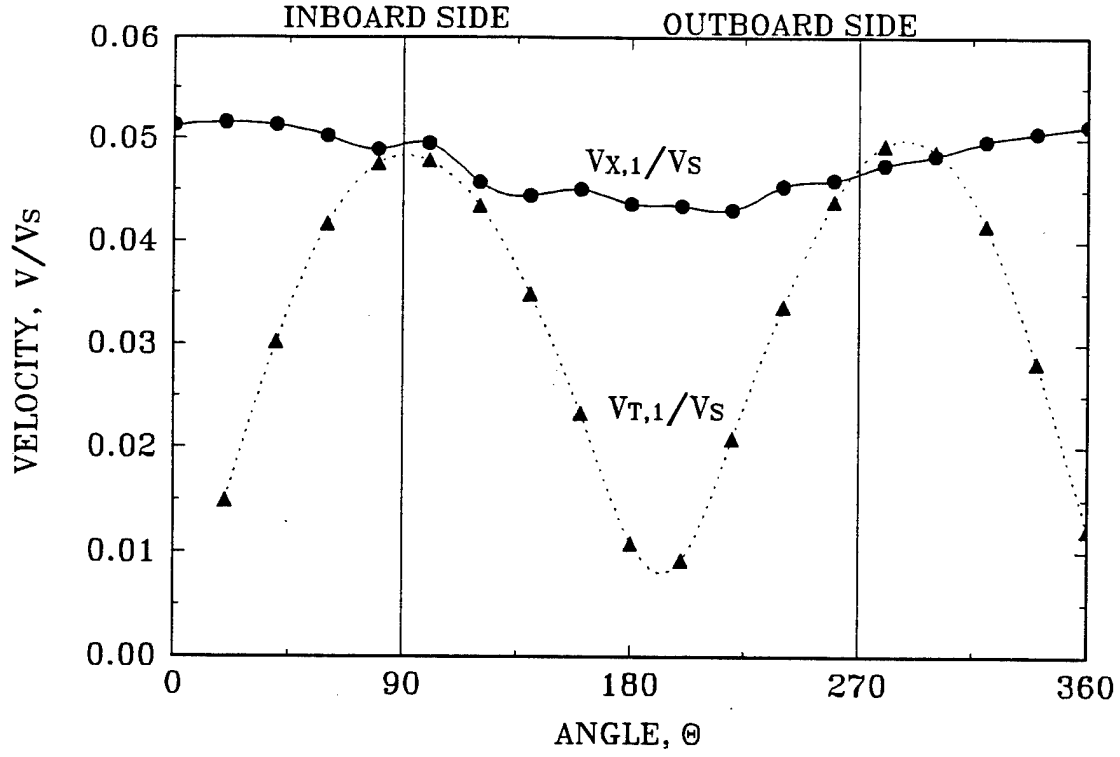

Fig 1. First Harmonic Perturbation Velocity in Propeller Plane at r/R=0.57 Due to Free Motion in a 1 Meter Wave Amplitude

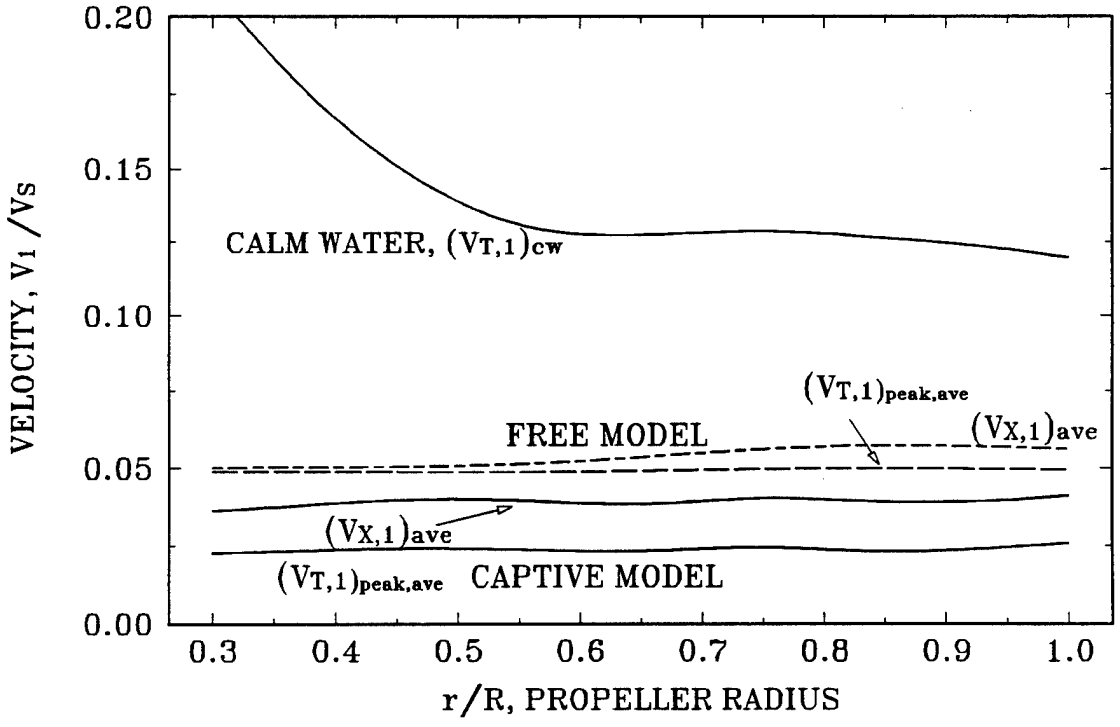

Fig 2. Perturbation Velocities due to 1 Meter Wave Amplitude

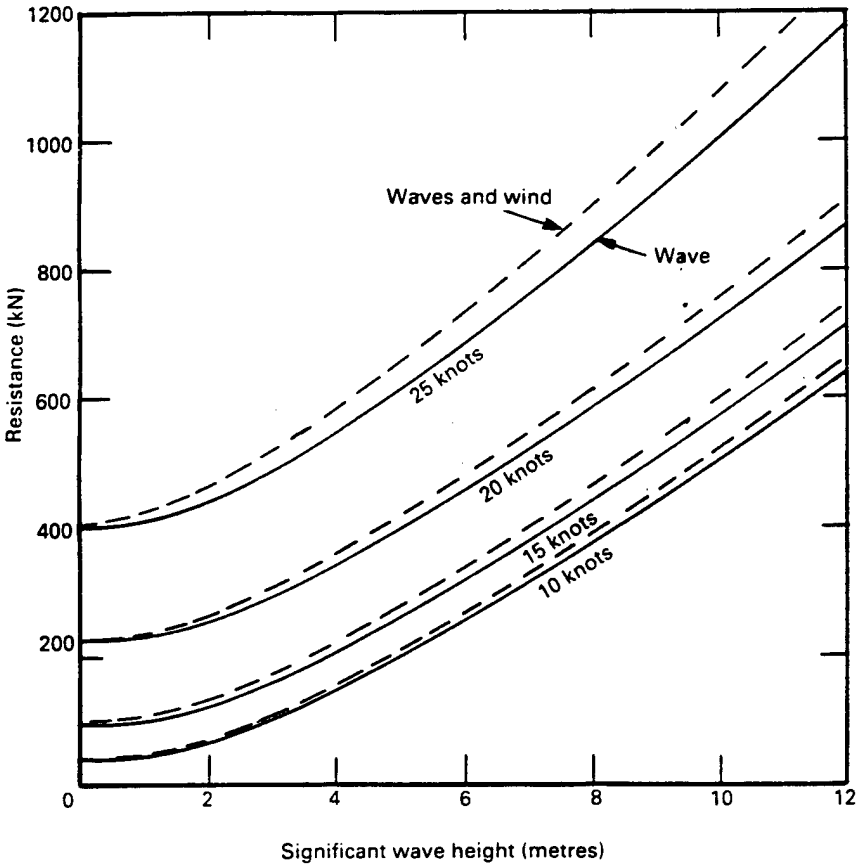

Fig 3. Resistance in Head Waves for a Frigate, From Lloyd[5]

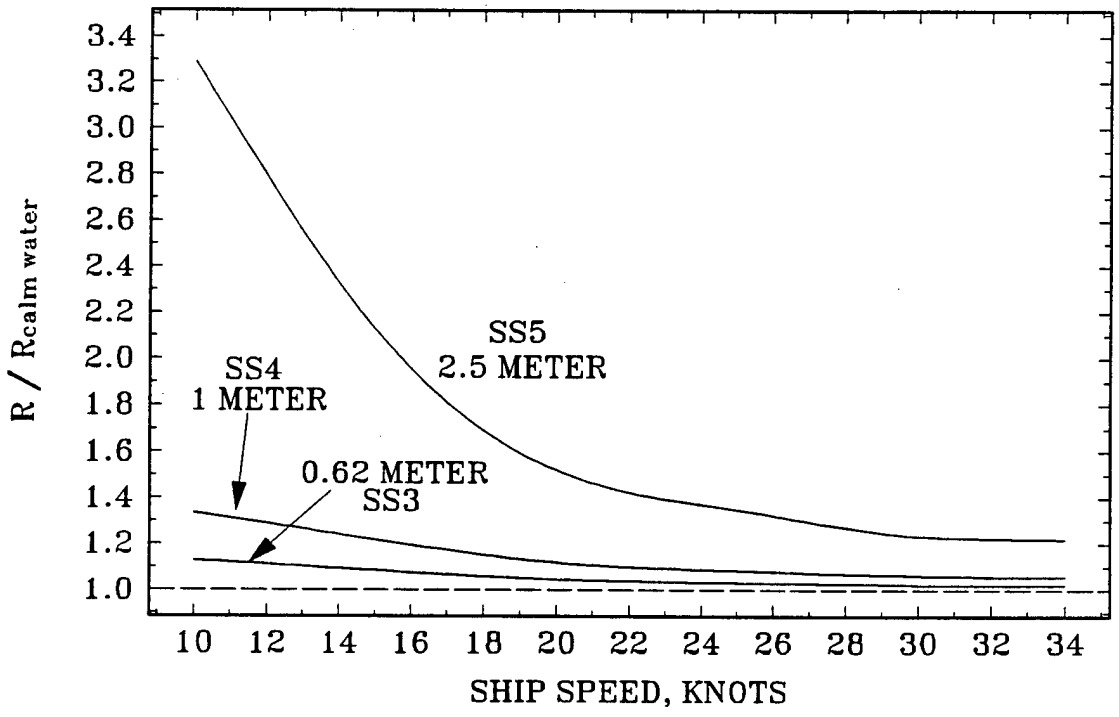

Fig 4. Estimated Increase in Resistance from Lloyd[5] data

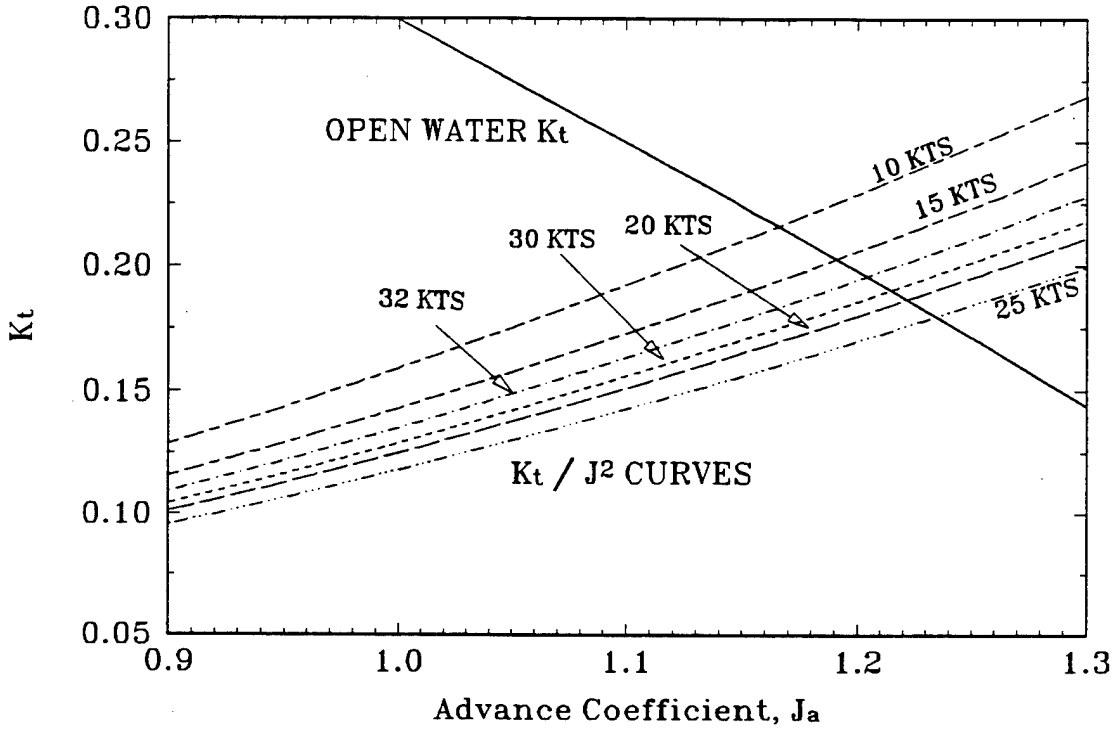

Fig 5. Determination of Propeller Advance Coefficient, J, in Sea State 3

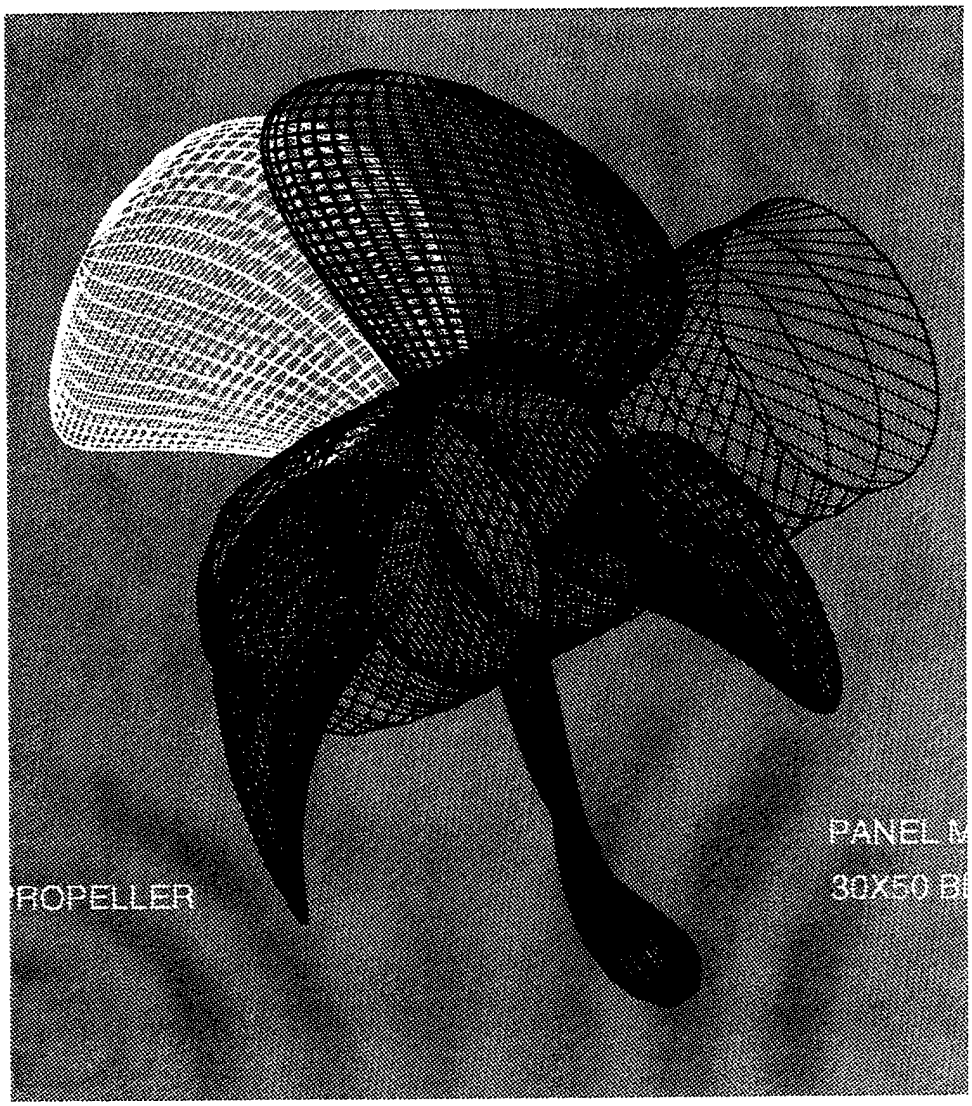

Fig 6. Propeller and Hub paneling for DD-963 Propeller

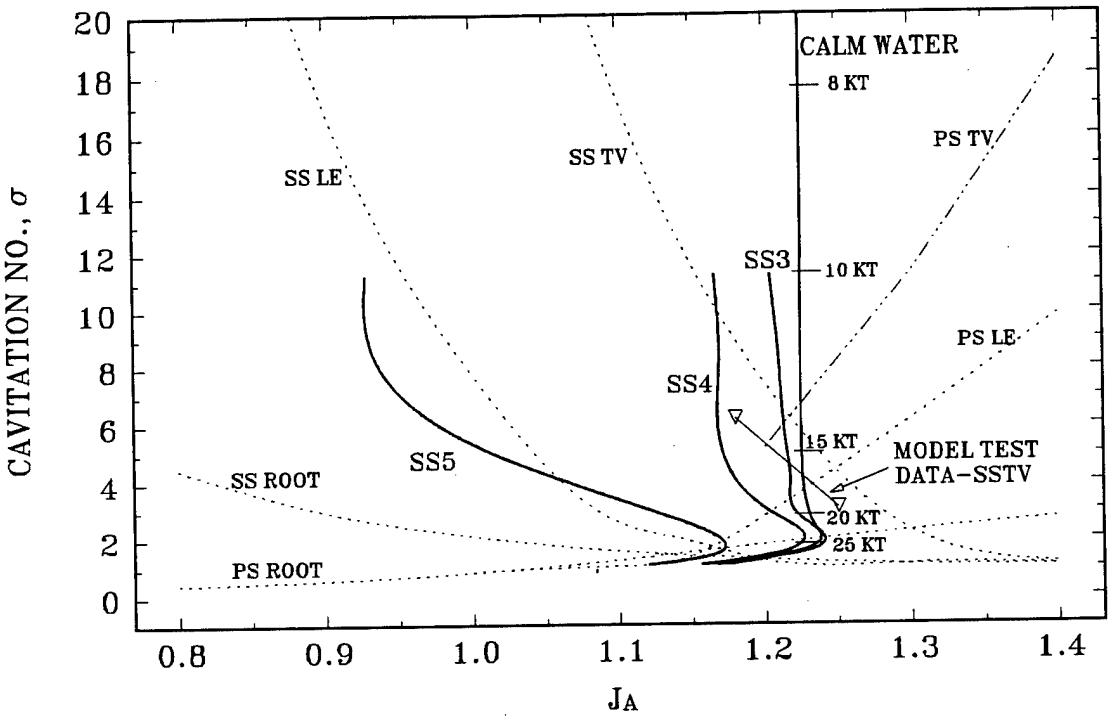

Fig 7. Cavitation Inception Prediction for Added Resistance in a Seaway

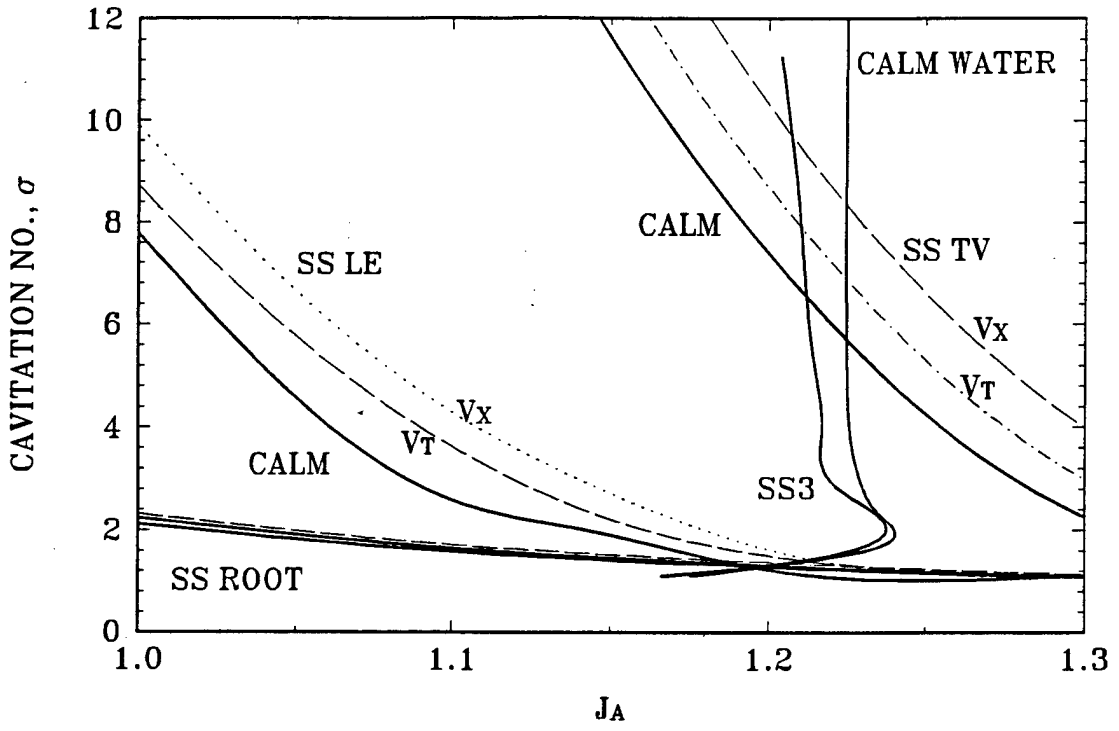

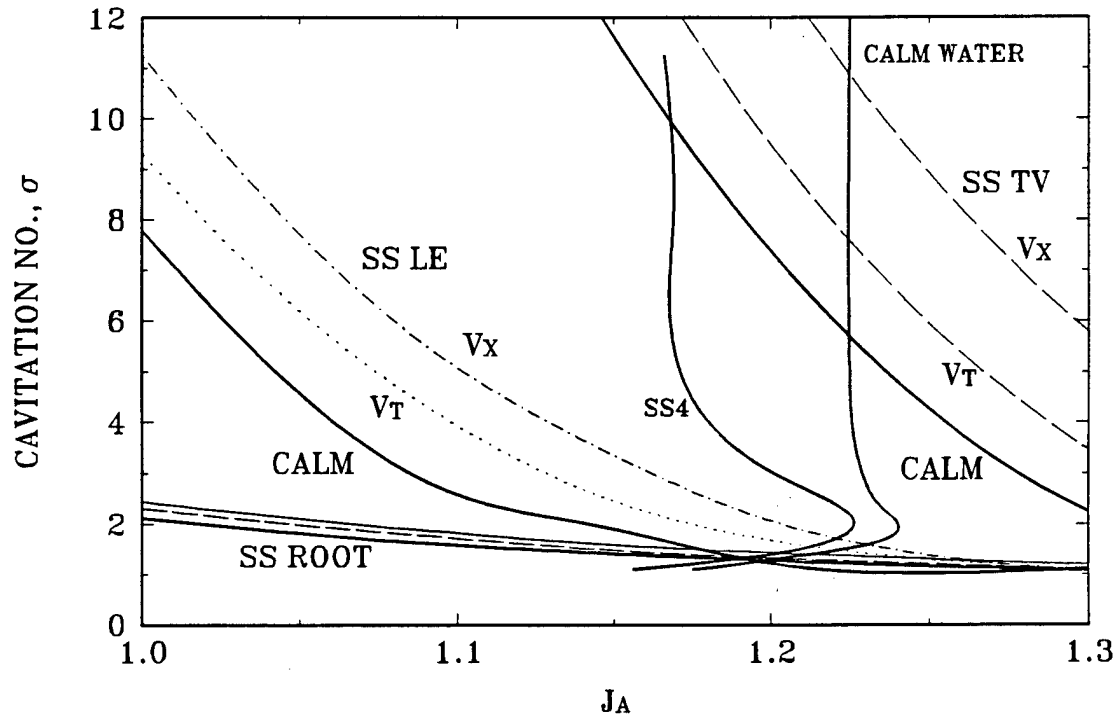

Fig 8. Cavitation Inception Prediction in Sea States 3 and 4

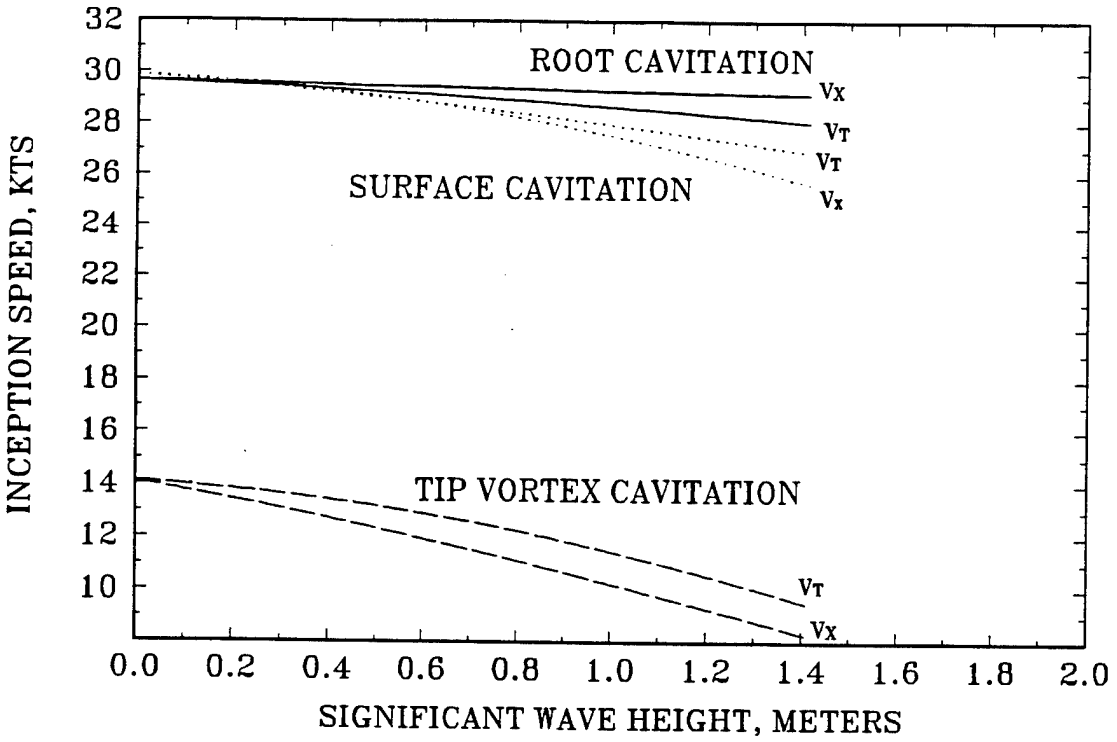

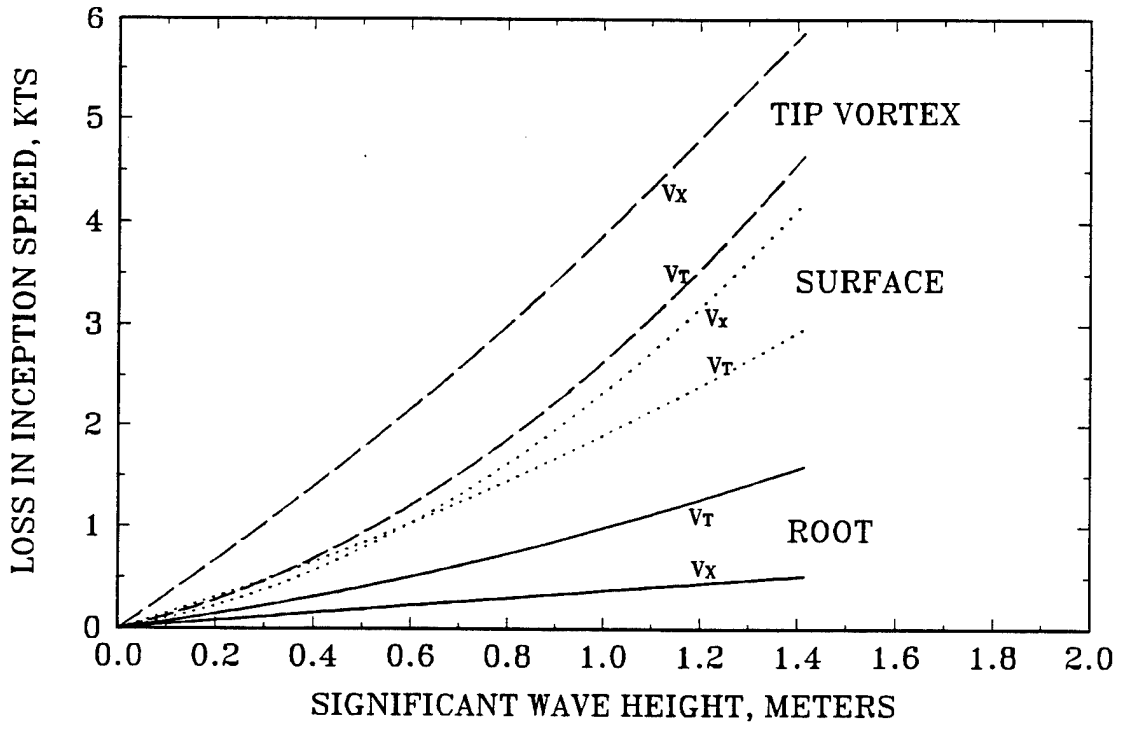

Fig 9. Predicted Cavitation Inception Speeds for increasing Significant Wave Height

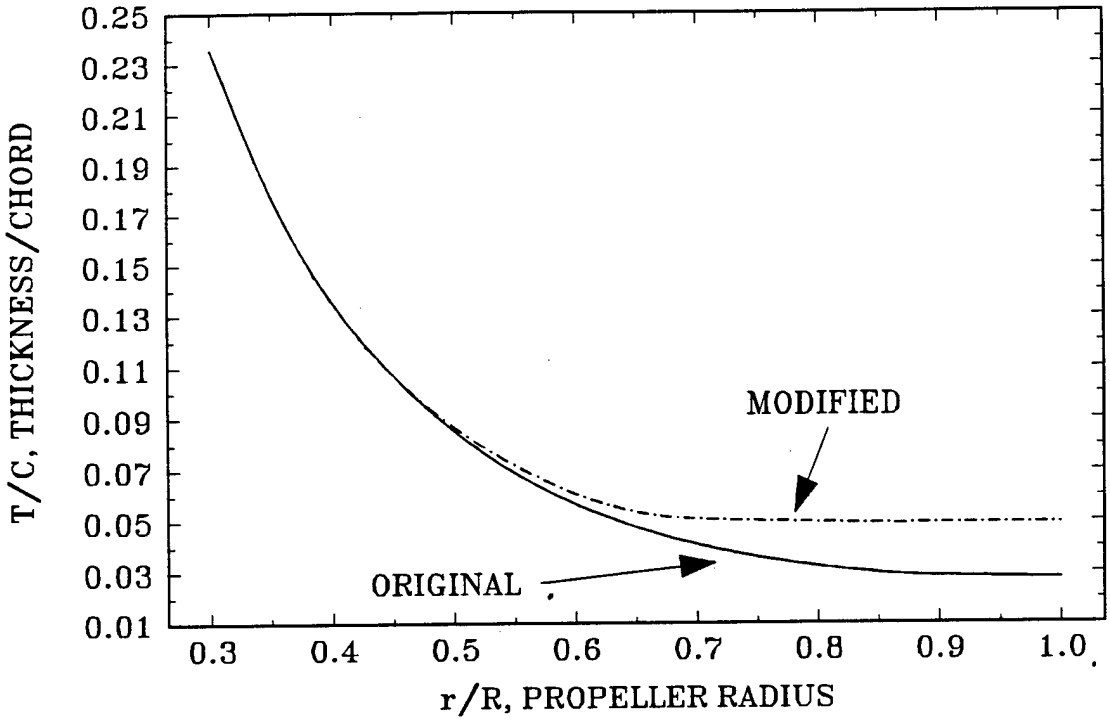

Fig 10. Modification of Propeller Blade Thickness

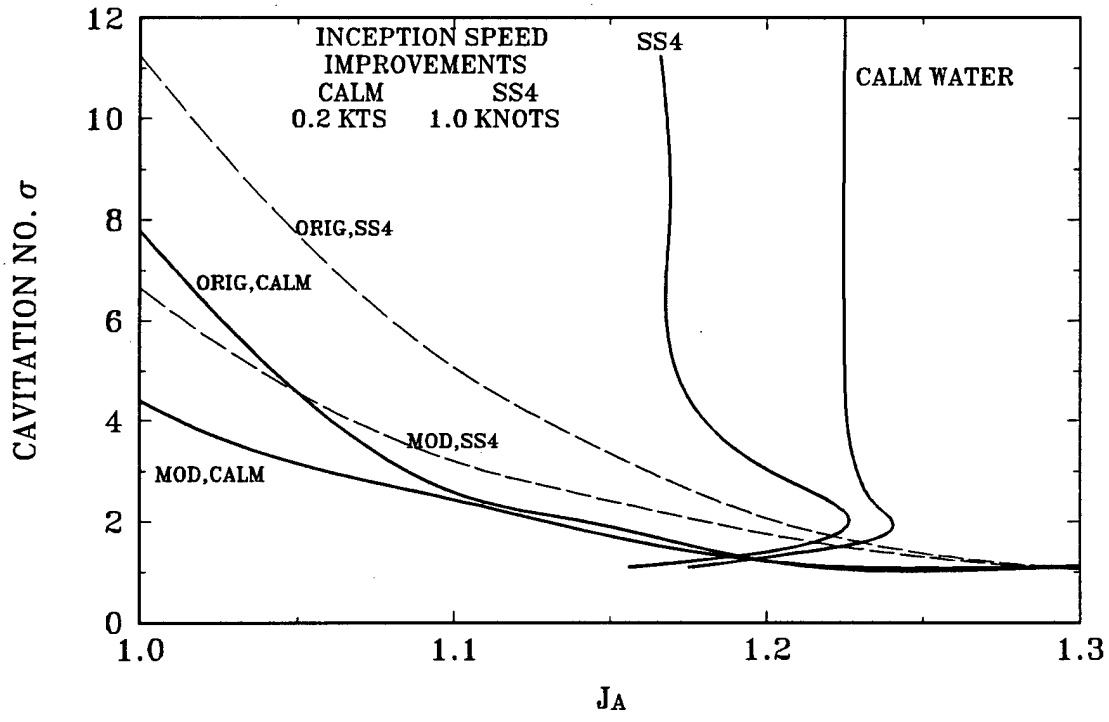

Fig 11. Predicted Improvement in Cavitation Inception Speed with modified Propeller Geometry

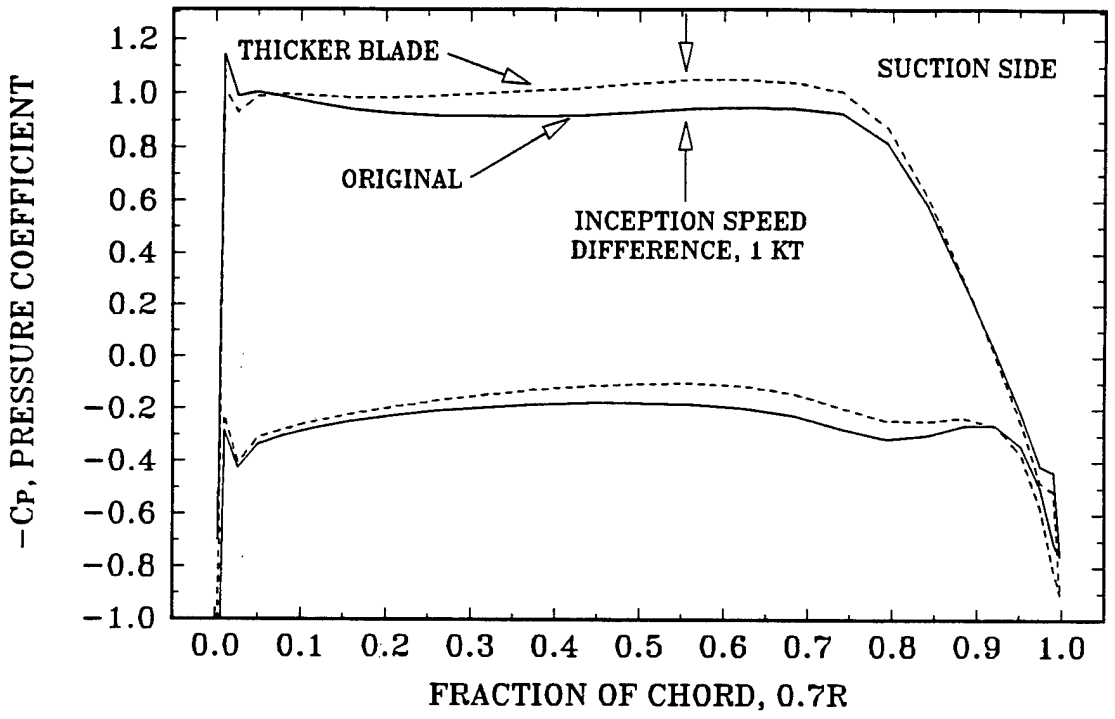

Fig 12. Predicted Blade pressure distribution at Maximum Loading for Original and Modified Geometry

Table 1 Calculated Harmonic Amplitude of Velocity at the propeller plane due to 1 meter regular wave with ship motion

Table 1a. Captive Model Case

Angle,θ	r/R=0.37		r/R=0.57		r/R=0.8		r/R=1.02	
deg.	$V_{x,1}$	ϕ_1	$V_{x,1}$	ϕ_1	$V_{x,1}$	ϕ_1	$V_{x,1}$	ϕ_1
0.,	0.038,	-146.	0.038,	-146.	0.039,	-145.	0.040,	-146.
20.,	0.038,	-146.	0.039,	-147.	0.040,	-148.	0.041,	-148.
40.,	0.038,	-147.	0.039,	-147.	0.040,	-148.	0.042,	-149.
60.,	0.038,	-147.	0.039,	-148.	0.040,	-149.	0.041,	-150.
80.,	0.038,	-147.	0.038,	-147.	0.039,	-148.	0.040,	-150.
100.,	0.038,	-146.	0.038,	-147.	0.038,	-148.	0.038,	-147.
120.,	0.037,	-146.	0.037,	-147.	0.037,	-147.	0.037,	-147.
140.,	0.036,	-147.	0.036,	-145.	0.036,	-146.	0.036,	-146.
160.,	0.036,	-147.	0.036,	-146.	0.035,	-146.	0.035,	-146.
180.,	0.035,	-149.	0.036,	-145.	0.035,	-145.	0.034,	-144.
200.,	0.035,	-146.	0.035,	-145.	0.034,	-145.	0.034,	-145.
220.,	0.036,	-146.	0.035,	-145.	0.035,	-144.	0.034,	-144.
240.,	0.036,	-144.	0.035,	-145.	0.035,	-146.	0.035,	-144.
260.,	0.036,	-145.	0.036,	-145.	0.036,	-144.	0.036,	-144.
280.,	0.036,	-145.	0.036,	-145.	0.036,	-144.	0.036,	-144.
300.,	0.037,	-145.	0.037,	-144.	0.037,	-144.	0.037,	-144.
320.,	0.038,	-145.	0.038,	-144.	0.038,	-144.	0.038,	-144.
340.,	0.038,	-144.	0.038,	-145.	0.038,	-145.	0.038,	-144.

Angle,θ	r/R=0.37		r/R=0.57		r/R=0.8		r/R=1.02	
deg.	$V_{r,1}$	ϕ_1	$V_{r,1}$	ϕ_1	$V_{r,1}$	ϕ_1	$V_{r,1}$	ϕ_1
0.,	-0.019,	113.	-0.018,	112.	-0.017,	110.	-0.015,	107.
20.,	-0.024,	118.	-0.025,	118.	-0.026,	118.	-0.028,	117.
40.,	-0.027,	122.	-0.029,	122.	-0.032,	122.	-0.036,	122.
60.,	-0.025,	125.	-0.027,	125.	-0.030,	126.	-0.033,	125.
80.,	-0.019,	130.	-0.020,	130.	-0.022,	130.	-0.024,	129.
100.,	-0.010,	139.	-0.010,	139.	-0.011,	137.	-0.011,	141.
120.,	-0.003,	-148.	-0.003,	-130.	-0.003,	-127.	-0.003,	-116.
140.,	-0.009,	-74.	-0.011,	-73.	-0.011,	-73.	-0.013,	-69.
160.,	-0.016,	-66.	-0.018,	-65.	-0.018,	-64.	-0.019,	-63.
180.,	-0.021,	-62.	-0.022,	-62.	-0.022,	-62.	-0.022,	-61.
200.,	-0.023,	-61.	-0.022,	-61.	-0.022,	-61.	-0.022,	-61.
220.,	-0.020,	-58.	-0.020,	-59.	-0.019,	-60.	-0.018,	-60.
240.,	-0.018,	-56.	-0.016,	-57.	-0.014,	-56.	-0.013,	-59.
260.,	-0.013,	-51.	-0.011,	-53.	-0.009,	-53.	-0.007,	-55.
280.,	-0.007,	-42.	-0.006,	-40.	-0.005,	-37.	-0.003,	-31.
300.,	-0.003,	15.	-0.003,	12.	-0.003,	24.	-0.003,	32.
320.,	-0.006,	87.	-0.006,	79.	-0.005,	65.	-0.004,	52.
340.,	-0.013,	106.	-0.011,	101.	-0.009,	93.	-0.007,	80.

Table 1a (continued)

Angle,θ	r/R=0.37		r/R=0.57		r/R=0.8		r/R=1.02	
deg.	$V_{t,1}$	ϕ_1	$V_{t,1}$	ϕ_1	$V_{t,1}$	ϕ_1	$Vt_{,1}$	ϕ_1
0.,	0.015,	132.	0.017,	131.	0.019,	130.	0.023,	129.
20.,	0.009,	146.	0.011,	142.	0.014,	139.	0.018,	137.
40.,	0.004,	-131.	0.004,	-147.	0.005,	-165.	0.005,	-175.
60.,	0.011,	-75.	0.012,	-75.	0.013,	-76.	0.014,	-74.
80.,	0.020,	-66.	0.021,	-65.	0.023,	-64.	0.024,	-63.
100.,	0.025,	-61.	0.027,	-61.	0.028,	-60.	0.030,	-60.
120.,	0.026,	-59.	0.027,	-58.	0.028,	-58.	0.029,	-57.
140.,	0.024,	-56.	0.024,	-56.	0.025,	-55.	0.024,	-55.
160.,	0.017,	-51.	0.018,	-53.	0.017,	-53.	0.017,	-52.
180.,	0.010,	-45.	0.009,	-45.	0.008,	-44.	0.008,	-44.
200.,	0.003,	-10.	0.002,	10.	0.002,	46.	0.002,	76.
220.,	0.006,	95.	0.008,	100.	0.008,	105.	0.009,	109.
240.,	0.012,	108.	0.013,	110.	0.013,	111.	0.014,	112.
260.,	0.017,	113.	0.016,	113.	0.016,	112.	0.015,	113.
280.,	0.019,	116.	0.018,	115.	0.016,	113.	0.015,	112.
300.,	0.021,	118.	0.019,	117.	0.017,	115.	0.015,	113.
320.,	0.021,	121.	0.020,	121.	0.018,	120.	0.016,	118.
340.,	0.019,	125.	0.020,	126.	0.020,	125.	0.019,	125.

Table 1b. Free Model Case

Angle,θ	r/R=0.37		r/R=0.57		r/R=0.8		r/R=1.02	
deg.	$V_{x,1}$	ϕ_1	$V_{x,1}$	ϕ_1	$V_{x,1}$	ϕ_1	$V_{x,1}$	ϕ_1
0.0	0.0502	-154.2	0.0513	-156.2	0.0503	-155.7	0.0543	-156.3
20.0	0.0500	-156.2	0.0516	-156.4	0.0535	-156.7	0.0555	-157.0
40.0	0.0498	-156.3	0.0514	-156.8	0.0569	-155.0	0.0561	-157.7
60.0	0.0493	-156.4	0.0503	-156.7	0.0519	-157.4	0.0525	-158.8
80.0	0.0484	-156.4	0.0490	-156.7	0.0512	-155.8	0.0506	-157.5
100.0	0.0477	-155.1	0.0496	-155.2	0.0476	-156.8	0.0457	-157.9
120.0	0.0465	-156.2	0.0458	-156.3	0.0454	-156.5	0.0450	-156.3
140.0	0.0459	-156.0	0.0445	-156.2	0.0437	-155.3	0.0428	-156.4
160.0	0.0457	-155.8	0.0451	-159.2	0.0428	-155.9	0.0416	-156.0
180.0	0.0452	-154.9	0.0437	-155.7	0.0424	-155.7	0.0398	-155.1
200.0	0.0450	-156.9	0.0435	-156.8	0.0424	-157.0	0.0413	-155.4
220.0	0.0458	-155.4	0.0431	-153.1	0.0471	-152.4	0.0422	-155.1
240.0	0.0439	-155.1	0.0454	-155.3	0.0449	-155.4	0.0436	-154.9
260.0	0.0465	-155.3	0.0460	-155.0	0.0458	-155.0	0.0460	-153.9
280.0	0.0475	-155.5	0.0475	-155.3	0.0474	-155.0	0.0475	-154.9
300.0	0.0481	-155.4	0.0484	-155.2	0.0489	-155.1	0.0494	-154.9
320.0	0.0491	-154.4	0.0498	-154.2	0.0504	-155.3	0.0510	-155.2
340.0	0.0481	-152.9	0.0506	-155.8	0.0517	-155.7	0.0527	-155.7

Table 1b (continued)

Angle,θ	r/R=0.37		r/R=0.57		r/R=0.8		r/R=1.02	
deg.	$V_{r,1}$	ϕ_1	$V_{r,1}$	ϕ_1	$V_{r,1}$	ϕ_1	$V_{r,1}$	ϕ_1
0.0	-0.0511	93.6	-0.0527	93.0	-0.0547	93.3	-0.0570	91.7
20.0	-0.0439	98.6	-0.0447	99.1	-0.0456	99.6	-0.0465	100.3
40.0	-0.0320	107.0	-0.0320	109.0	-0.0307	115.4	-0.0324	115.1
60.0	-0.0180	126.0	-0.0182	131.1	-0.0198	137.7	-0.0196	142.2
80.0	-0.0100	-167.0	-0.0112	-164.3	-0.0142	-158.3	-0.0140	-162.5
100.0	-0.0195	-113.3	-0.0199	-113.9	-0.0203	-115.5	-0.0216	-116.7
120.0	-0.0313	-98.4	-0.0306	-97.5	-0.0302	-98.2	-0.0291	-98.2
140.0	-0.0406	-92.2	-0.0393	-91.2	-0.0377	-92.2	-0.0368	-89.6
160.0	-0.0455	-87.8	-0.0438	-87.3	-0.0425	-86.6	-0.0411	-86.3
180.0	-0.0458	-85.3	-0.0444	-84.5	-0.0430	-84.0	-0.0418	-82.1
200.0	-0.0414	-82.3	-0.0406	-82.4	-0.0397	-82.6	-0.0390	-82.4
220.0	-0.0321	-79.4	-0.0326	-78.8	-0.0320	-81.2	-0.0317	-81.7
240.0	-0.0189	-70.5	-0.0194	-74.2	-0.0200	-78.6	-0.0206	-80.2
260.0	-0.0061	-14.5	-0.0057	-28.3	-0.0055	-47.7	-0.0053	-58.8
280.0	-0.0156	72.7	-0.0157	72.9	-0.0144	74.9	-0.0129	78.4
300.0	-0.0325	82.3	-0.0326	82.6	-0.0324	83.8	-0.0321	84.5
320.0	-0.0449	86.6	-0.0463	86.4	-0.0461	84.8	-0.0488	85.8
340.0	-0.0514	90.8	-0.0534	89.2	-0.0557	88.2	-0.0581	87.5

Angle,θ	r/R=0.37		r/R=0.57		r/R=0.8		r/R=1.02	
deg.	$V_{t,1}$	ϕ_1	$V_{t,1}$	ϕ_1	$V_{t,1}$	ϕ_1	$Vt_{,1}$	ϕ_1
0.0	0.0145	-124.8	0.0149	-130.4	0.0142	-123.3	0.0178	-130.8
20.0	0.0284	-105.0	0.0302	-106.3	0.0324	-107.8	0.0348	-109.3
40.0	0.0404	-96.5	0.0417	-97.3	0.0461	-100.8	0.0446	-99.0
60.0	0.0471	-91.2	0.0476	-90.9	0.0476	-91.4	0.0480	-90.4
80.0	0.0483	-86.2	0.0479	-85.4	0.0497	-86.5	0.0469	-83.3
100.0	0.0443	-81.7	0.0435	-80.4	0.0425	-79.0	0.0415	-76.5
120.0	0.0358	-76.7	0.0349	-75.3	0.0339	-73.4	0.0333	-72.0
140.0	0.0239	-68.7	0.0233	-67.2	0.0237	-63.7	0.0221	-64.9
160.0	0.0109	-46.3	0.0108	-44.1	0.0106	-44.1	0.0108	-42.2
180.0	0.0105	45.2	0.0092	51.9	0.0078	50.5	0.0070	57.0
200.0	0.0221	78.6	0.0208	79.8	0.0195	80.6	0.0184	81.5
220.0	0.0355	86.7	0.0337	86.5	0.0331	88.4	0.0315	89.6
240.0	0.0448	90.1	0.0439	90.4	0.0430	90.7	0.0420	91.5
260.0	0.0492	92.1	0.0494	91.7	0.0492	91.8	0.0493	91.5
280.0	0.0479	93.9	0.0488	93.2	0.0499	92.6	0.0508	91.8
300.0	0.0402	97.7	0.0416	96.0	0.0433	94.5	0.0452	93.0
320.0	0.0271	105.1	0.0282	103.1	0.0315	102.1	0.0312	98.3
340.0	0.0112	125.9	0.0121	133.9	0.0123	132.2	0.0127	129.8

Table 2 Propeller Panel Method Calculation - Typical Summary Output

Received from MIT 6/1/93
Local Drag Coefficients added 1/18/94
Modified by Jim Bailar on or after 6/17/93
PROP 4661 J=1.1 VT- VX+B UNSTEADY WAKE JUNE 6,1995

ADVCO	CUT	NBLADE	NC	NR	MTIP	ITHK
1.1000	1.0000	5	50	30	0	8

R/RO	P/D	XS/D	SKEW	C/D	FO/C	to/c	CDrag	VX	VR	VT	UANW	UTNW	UAUW	UTUW
0.300	1.1650	0.0096	2.985	0.1780	0.0000	0.2360	0.0070	1.050	0.000	-0.209	-0.050	-0.026	0.139	-0.273
0.350	1.2960	0.0123	3.481	0.2100	0.0050	0.1771	0.0000	1.050	0.000	-0.186	-0.039	-0.076	0.105	-0.162
0.450	1.4800	0.0186	4.810	0.2710	0.0209	0.1070	0.0000	1.050	0.000	-0.151	0.037	-0.172	0.143	-0.110
0.550	1.5660	0.0266	6.631	0.3270	0.0267	0.0691	0.0000	1.051	0.000	-0.131	0.140	-0.239	0.229	-0.165
0.650	1.5660	0.0356	8.978	0.3740	0.0256	0.0476	0.0000	1.053	0.000	-0.128	0.214	-0.252	0.248	-0.184
0.750	1.4980	0.0447	11.895	0.4060	0.0209	0.0360	0.0000	1.056	0.000	-0.129	0.230	-0.210	0.178	-0.125
0.850	1.3810	0.0532	15.410	0.4090	0.0151	0.0298	0.0000	1.058	0.000	-0.126	0.179	-0.137	0.092	-0.052
0.900	1.3060	0.0567	17.403	0.3870	0.0122	0.0284	0.0000	1.058	0.000	-0.125	0.127	-0.097	0.068	-0.032
0.950	1.2220	0.0596	19.557	0.3260	0.0094	0.0279	0.0000	1.058	0.000	-0.123	0.057	-0.060	0.069	-0.033
1.000	1.1280	0.0615	21.876	0.0000	0.0000	0.0000	0.0000	1.057	0.000	-0.120	-0.032	-0.028	0.106	-0.066

---------- SINGLE BLADE FORCE BY PRESSURE INTEGRATION (SUCTION = 0) (PARTIAL TABLE)----------

M	RP/RO	100 BKFX	100 BKMX	BCL	BCDP	100 BKMZ	100 CIRC
1	0.312	-0.0045	-0.0029	-0.0025	-0.0057	0.0015	-0.2212
3	0.358	-0.0020	0.0059	0.0061	0.0046	0.0012	-0.0087
5	0.405	-0.0765	0.0466	0.0482	0.0122	0.0301	0.4086
7	0.452	-0.2102	0.1134	0.0915	0.0176	0.0898	0.8824
9	0.498	-0.3787	0.1975	0.1237	0.0215	0.1761	1.3206
11	0.545	-0.5598	0.2886	0.1424	0.0235	0.2819	1.6760
13	0.592	-0.7352	0.3762	0.1493	0.0235	0.3985	1.9292
15	0.638	-0.8887	0.4499	0.1470	0.0217	0.5160	2.0725
17	0.685	-1.0053	0.5007	0.1380	0.0187	0.6230	2.1076
19	0.732	-1.0710	0.5209	0.1243	0.0149	0.7062	2.0293
21	0.778	-1.0751	0.5070	0.1077	0.0109	0.7518	1.8547
23	0.825	-1.0079	0.4575	0.0894	0.0073	0.7447	1.5878
25	0.872	-0.8613	0.3730	0.0700	0.0042	0.6698	1.2355
27	0.918	-0.6334	0.2597	0.0502	0.0018	0.5172	0.8120
29	0.965	-0.3072	0.1191	0.0278	0.0005	0.2770	0.2937
30	0.988	-0.0980	0.0370	0.0069	0.0009	0.1096	-0.0398
SUM		-0.1762	0.0842	0.1157			

BKT,VBKT, HKT,VHKT	0.1332	-0.0065	0.0015	-0.0020
BKQ,VBKQ, HKQ,VHKQ	0.0318	0.0039	0.0000	0.0002

DTMB DRAG	KT=	0.1333	KQ=	0.03203	ETAO= 0.7288
Cf=0.0000	KT=	0.1347	KQ=	0.03189	ETAO= 0.7394
Cf=0.0035	KT=	0.1262	KQ=	0.03597	ETAO= 0.6142
Cf=0.0070	KT=	0.1177	KQ=	0.04005	ETAO= 0.5144
Cf=0.0100	KT=	0.1104	KQ=	0.04355	ETAO= 0.4438